Preliminary Assessment of As-Built Design Characteristics for the Transformational Challenge Reactor

B. J. Ade[1], E. Biondo, D. P. Schappel, E. Fountain, B. R. Betzler, and G. Davidson

[1]Oak Ridge National Laboratory
One Bethel Valley Road, Oak Ridge, TN, 37831

adebj@ornl.gov

doi.org/10.13182/PHYSOR22-37829

ABSTRACT

The Transformational Challenge Reactor design effort in 2021 included constructing a full-core mock-up of the reactor in-core components. This effort was undertaken to ascertain differences between the as-designed and as-built individual components and determine impacts of assembly of the as-built components into a full-scale core assembly. Through this effort, several deviations from as-designed components were observed. Some of these deviations were related to the additive manufacturing processes, and others were related to deviations in traditionally manufactured components. The tolerance stack-up of these minor deviations was evaluated and quantified. A new layered geometry capability in Shift (CAD + combinatorial) was used to model variations in the placement of YH moderator rods, and the effects of this variation on k_{eff} and power distribution are analyzed in this paper. Bison was used to model the thermomechanical effect of contact between adjacent fuel elements.

KEYWORDS: additive manufacturing, 3D printing, TRISO, yttrium hydride, microreactor

1. INTRODUCTION

The Transformational Challenge Reactor (TCR) program is leveraging advances in several scientific areas—including materials, manufacturing, sensors and control systems, data analytics, and high-fidelity modeling and simulation—to accelerate the design, manufacturing, qualification, and deployment of advanced nuclear energy systems. From the program's inception, one core component of the program was to design, build, and operate a small nuclear reactor. The direction of the program has since changed and is no longer pursuing the construction of a fueled nuclear system. In lieu of a nuclear test, a full-core mock-up was constructed to ascertain the properties of a core composed of hundreds additively and traditionally manufactured components as it relates to reactor design.

A summary of the candidate core designs for this reactor was provided in *PHYSOR2020* [1]. The TCR design was advanced, and a preliminary design report was completed in 2020. Following the candidate core design work presented in *PHYSOR2020* [1], an update summarizing the TCR preliminary design is provided in these proceedings [2], the details of which are not repeated here. Instead, this paper focuses on the deviation from as-designed components observed in constructed components and the neutronic and thermomechanical analyses associated with the worst-case impacts of these deviations.

Although additive manufacturing (AM) has advantages over traditional manufacturing (e.g., complex geometry, rapid prototyping, online part monitoring), the AM process can result in deviations that are different than those typical in traditional manufacturing technologies. Variations in additively manufactured components compared with as-designed models vary with the technology being used. Large-scale processes tend to result in larger-scale deviations from the design and higher surface roughness, whereas small-scale processes tent to yield smaller deviations from the as-designed components and lower relative surface roughness. The technologies to detect these as-printed variations are being developed through process monitoring and machine learning techniques in separate efforts under the TCR program.

2. OBSERVED COMPONENT DEVIATIONS

2.1. Fuel Elements and Assemblies

The TCR fuel elements combine conventionally fabricated tristructural isotropic (TRISO) particle fuel with an additively manufactured SiC fuel container or shell that includes integrated cooling channels. The SiC shell is printed using a binder jet process. TRISO particles are poured into this fuel can, and additional SiC powder is then used to fill interstitial space in the element, after which the whole element undergoes chemical vapor infiltration (CVI) to solidify the element. The details of this process are provided in Terrani et al. [3]. This process yields a fuel element with high packing fraction (~60%) with internal coolant channels [3]. Postproduction examination of the TCR fuel elements indicates that they deviate from the designed elements, as shown in Figure 6 of Terrani et al. [3]. Because of the current limited throughput of the CVI process, plastic surrogate fuel elements are used in the full-core mock-up. These elements were printed using a powder-based process call multi jet fusion (MJF) to represent SiC elements as accurately as possible. Binder jet and MJF are both powder-based processes, hence the choice of MJF instead of a filament-based printing process.

Upon completion of the surrogate fuel elements, inspection and qualitative measurements indicated deviations from the as-designed components. In particular, the sides of the surrogate fuel elements are not perpendicular to the bottom surface of the elements. Eleven surrogate fuel elements were selected from two different production batches, and the amount of deviation at the top of the surrogate fuel element tip relative to the bottom was measured. That is, the bottom of one fuel element tip was placed at a consistent location, and then then tilt of that side of the element was measured. The measured deviations for these 11 elements vary up to a maximum of 0.7 mm along the height of the element. The standard deviation of these measurements is ~0.3 mm. The deviations in actual fuel element is expected to be smaller than those measured in the surrogate elements, and major parameters, such as fuel and coolant volumes are not expected to deviate significantly.

The worst stacking of these elements could yield large deviations along the length of the fuel assemblies, so some mitigation of these deviations was pursued. The TCR mock-up assemblies contain eight full-sized fuel elements and two integrated axial reflectors that are identical to the design of the fuel elements. In the nuclear core, the bottom eight elements are filled with TRISO, whereas the top two elements are filled with SiC. However, because the fuel element and top axial reflector elements are of the same design, 10 elements compose one fuel assembly. These 10 (N) elements can be arranged in any order, and each element can be

arranged in three rotational orientations (R). The total number of different stacking arrangements that can then be constructed from 10 selected elements is given by Eq. (1):

$$N! \times R^{N-1}. \quad (1)$$

For 10 elements and three rotations per element, ~71 billion different assembly configurations can be achieved.

To test the different stacking orders and orientations, a simple Monte Carlo–based algorithm was developed to simulate fuel element stacking. The algorithm first selects 10 of the 11 fuel elements measured and then selects one of three possible orientations for each fuel element. For each iteration, the maximum expected deviation is recorded and saved. Ten million iterations were performed, and the best and worst stacking orientations were selected for assembly with the surrogate fuel elements. Images of these two different configurations are provided in Figure 1, which shows the worst and best assembly configurations as compared with a known straight edge.

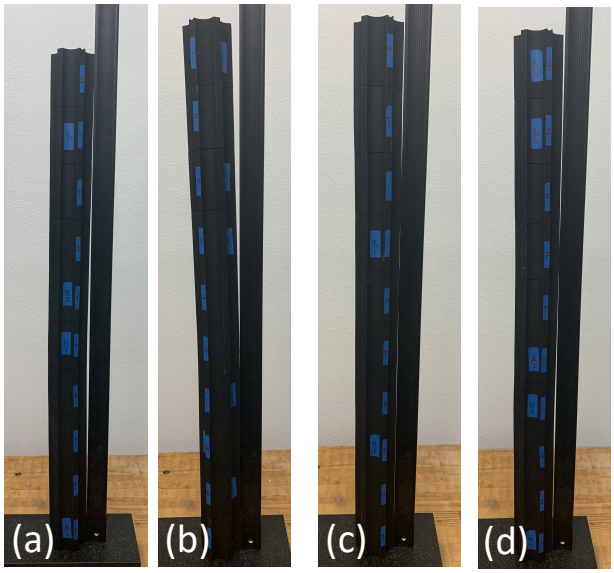

Figure 1. Opposite sides of the worst predicted assembly configuration (a and b) and opposite sides of the best predicted assembly configuration (c and d). The gap in (a) appears significantly smaller than the gap in (b) because the straight edge is contacting both the top and bottom of the stack, whereas (b) is only contacting the bottom of the stack.

The images in Figure 1 clearly indicate that the order and stacking orientation (i.e., rotation) selected can significantly affect the straightness of the completed assembly. As expected, the poor stacking orientations are those in which the deviations all align in the same direction, and the best stacking orientations are those that alternate the negative and positive deviations along the length of the assembly. For the full-core mock-up, measuring each of the 432 surrogate fuel elements and following computational optimization was intractable. In practice, the central moderator tube is used as a guide while stacking the elements. If the central moderator tube is not visually centered in the fuel element, then the rotation can be changed to provide a more consistent gap between the moderator tube and the fuel element.

As a result of the fuel element deviations from their as-designed state, the gap between the neighboring fuel assemblies and between the moderator rods and the fuel element varies. This variation leads to contact between some fuel elements and larger gaps designed between other fuel elements. This also leads to size variations in the gap between the moderator rods and the fuel elements.

2.2. Bottom Reflector Elements

The bottom reflector elements in the TCR design are made in a manner similar to the fuel elements; however, these elements are solid SiC. First, an empty shell is printed; then, the shell is filled with SiC powder, and the entire element undergoes CVI to solidify the element. The bottom reflector elements nestle into mating features in the bottom support plate, and the fuel assemblies and free moderator rods are stacked atop these bottom reflector elements. A graphic showing the bottom reflectors and the support plate is provided in Figure 2a. The reflector elements printed for the TCR full-core mock-up deviated significantly from the as-designed components, as shown in Figure 2b. The bowing along the bottom reflector elements was apparent for both the fuel assembly reflectors and the free moderator rod reflectors, even though they are simpler geometrically (i.e., a cylinder with a taper at the bottom and top).

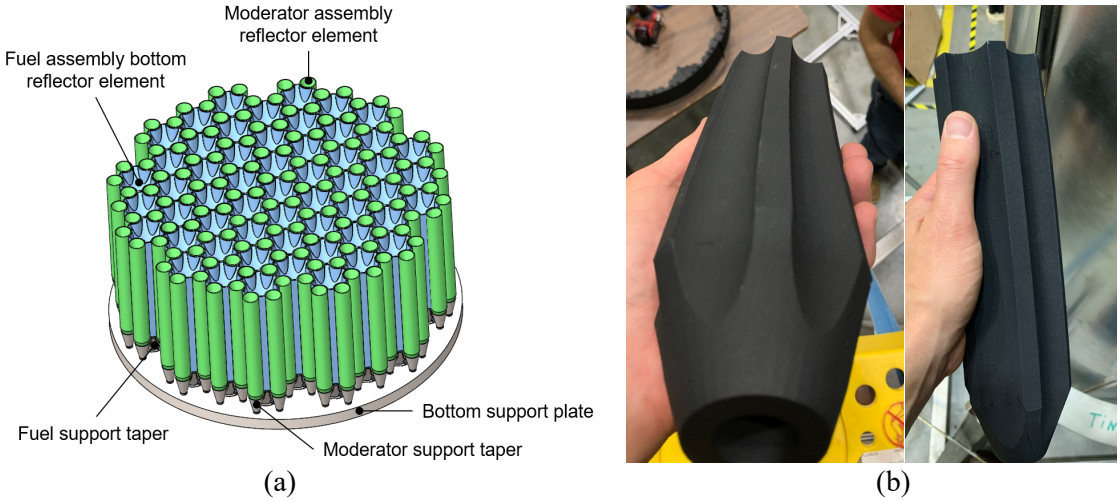

Figure 2. (a) The bottom reflector elements fully loaded onto the bottom support plate tapers; the blue reflector elements support the fuel assemblies, and the green elements support the free moderator rods. (b) The surrogate bottom fuel assembly reflector element bowing.

The effect of the bowing is twofold: (1) the top mating surface is out of plane compared with the bottom mating surface, and (2) the centerline of the bottom taper and the top recess no longer aligns. This results in the fuel assemblies and free moderator rods tilting during the assembly of the mock-up core. This is not a significant issue for the fuel assemblies because the fuel element tips contact one another in adjacent fuel assemblies, resulting in the self-alignment of the fuel assemblies in a relatively consistent pattern. However, some of the free moderator rods tilt to the point of contact with the fuel elements at the top of the core. These free moderator rods are not assumed to contact along the entire length of the fuel assembly because the taper in the bottom reflector forces better spacing at the bottom of the core.

Figure 3 shows some of the observed deviations in the mock-up core; Figure 3a provides a top-down view on the entire core, and Figure 3b provides an enlarged view of a fuel single assembly and its neighboring free moderator rods. As shown in Figure 3b, the gaps between the fuel element vary with contact between some elements and larger gaps on opposing corners, and the free moderator rods are not all centered between the fuel assemblies. A top alignment plate is included in the TCR design and was constructed for the full-core mock-up whose purpose was to force rod alignment; however, the centering mechanism chosen does not apply sufficient force to align all the rods in the full-core mock-up. Regardless, during irradiation, the stainless-steel rods are expected to bow as a function of fluence and temperature variation, so inconsistencies in the fuel element spacing and free moderator rods required assessment.

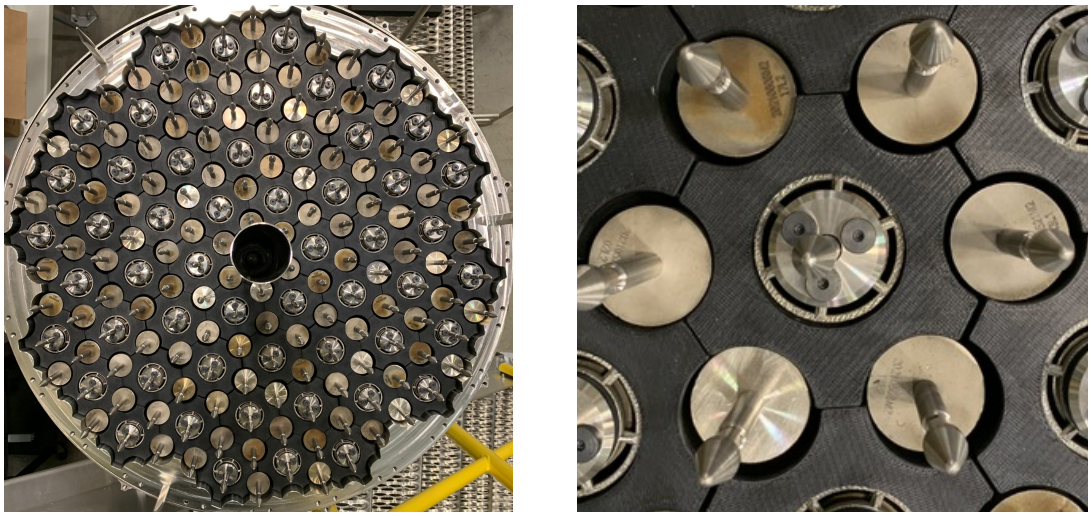

(a) (b)

Figure 3. (a) Top-down view of the TCR full-core mock-up. (b) Enlarged view of the top of a fuel assembly and its neighboring free moderator rods.

3. SIMULATION OF OBSERVED DEVIATIONS

Two of the observed deviations from the TCR design as observed in the TCR full-core mock-up were chosen for further analysis based on their expected effect on reactor performance. The first was neutronic modeling of the variation in the location of the free moderator rods. The spacing of the moderator rods is inconsistent, as shown in Figure 3. A newly developed layered geometry method developed in the Shift Monte Carlo code [4] in which CAD and combinatorial geometry can be combined was used to simulate random displacements in the free moderator rods and to compare the displacements with the nominal (i.e., as-designed) TCR geometry. The effect on k_{eff} and power distribution was analyzed.

Through previous TCR fuel element performance work [5] using Bison [6, 7], variation in the neutronic power distribution in the fuel elements resulted in relatively small changes to the stress distribution and failure probability. However, changes to the thermal boundary conditions in the Bison fuel element models will likely have larger impacts. For this reason, a different variation in the TCR geometry observed in the TCR full-core mock-up (i.e., fuel element contact) was analyzed. The contact between fuel element tips is not expected to cause large stresses because there is not coupling between the contact surfaces (i.e., they move independently). Instead, contact along one fuel element tip and a corresponding larger gap along the opposite fuel element tip cause variation in the fuel-to-coolant heat transfer coefficient (HTC). Contact between fuel element tips has an insulating effect and lowers the heat transfer coefficient; conversely, a larger gap along the opposite fuel element tip yields a higher heat transfer coefficient than the as-designed gap. The impact on fuel element stress for these conditions is analyzed using Bison.

3.1. Neutronic Simulations Results

For MC eigenvalue simulations, a base case model was first constructed using Shift's nascent *layered* geometry feature [4]. This was done by overlaying CAD models of fuel and integrated reflector elements upon a Shift constructive solid geometry (CSG) model containing moderator rods and the rest of the TCR geometry including bottom reflector, support plate, vessel, and radial reflector. The void space in the CAD models was declared “transparent”, allowing the moderator rods in the CSG model to occupy the central and interstitial spaces around CAD fuel element models.

Five additional trial models were created in the same manner as the as-designed case, each of which using randomly perturbed moderator rods. Moderator rods were perturbed by first sampling a rod displacement from [0, gap width] and then sampling a displacement direction from [0, 2π). An X-Y slice through the axial midplane of the trial 4 model and a zoomed image showing a close up of the moderator rod displacement are provide in Figure 4. In this assumption, the entire moderator rod is shifted to a new *X-Y* location within its channel. This is the worst-case assumption because moderator rods tilt rather than translate in the actual full core mock-up. This assumption effects the entire length of the fuel element stack rather than only a portion of the top element.

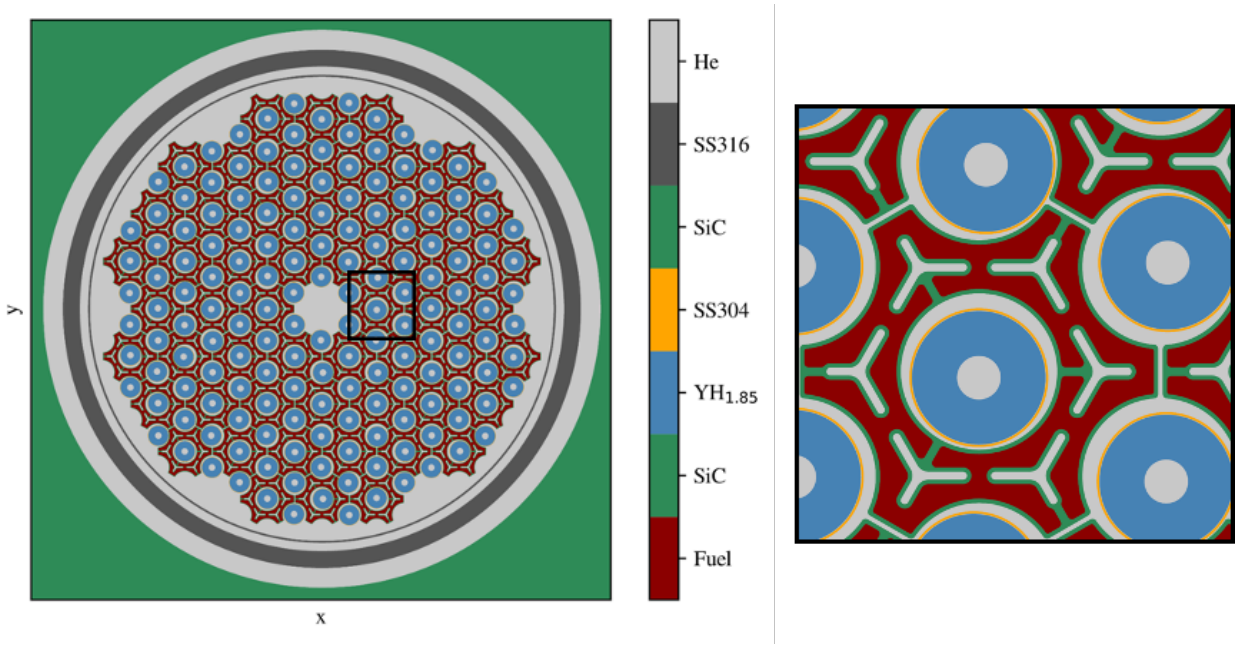

(a) (b)

Figure 4. (a) *X-Y* slice through the Shift TCR core model midplane and (b) magnified view of the displacement of the free moderator rods in the Shift model.

The as-designed Shift model with all moderator rods perfectly centered yielded a k_{eff} of 1.02123 ± 0.00010 (i.e., 5E6 particles per cycle for 25 inactive and 25 active cycles). The five random rod placement realizations yielded k_{eff} values of 1.02098, 1.02073, 1.02077, 1.02103, and 1.02119 with an average estimated standard deviation 0.00069. The new layered geometry method has not yet been optimized, and as a result, a significant amount of CPU time is required to generate the results, hence the larger estimated standard deviation on the random realizations. The average k_{eff} of these random realizations is 1.02094 ± 0.00019, indicating that the random moderator rod placement does not significantly affect k_{eff}.

The fifth random realization was then selected for further analysis and comparison with the nominal case. The fifth realization was selected because it provided the closest k_{eff} value to the nominal case. This case was then run using the same number of particles per cycle and active and inactive cycles to improve the k_{eff} and fission source distribution statistics. The updated k_{eff} for this case (1.02112 +/- 0.00014) provides further evidence that the random rod placement does not significantly affect k_{eff}. Figure 5 compares the fission source distributions for the nominal case and the fifth realization over a fine *X-Y* mesh. The results in Figure 5 indicate that areas in which the moderator rods cluster toward one another yield an increase in the fission source over the nominal case by up to 5%. Conversely, when the moderator rods all lean away from the fuel elements in one area, a reduction in the fission source by up to 5% is observed. It is feasible that this entire range of variation in power over one fuel element results in a 10% power tilt across a fuel element. Again, this is likely much larger than is truly feasible because this is a worst-case scenario in which the top

alignment plate is assumed to provide no additional alignment, and in the constructed mock-up, a lean of the moderator rods is observed rather than a translation.

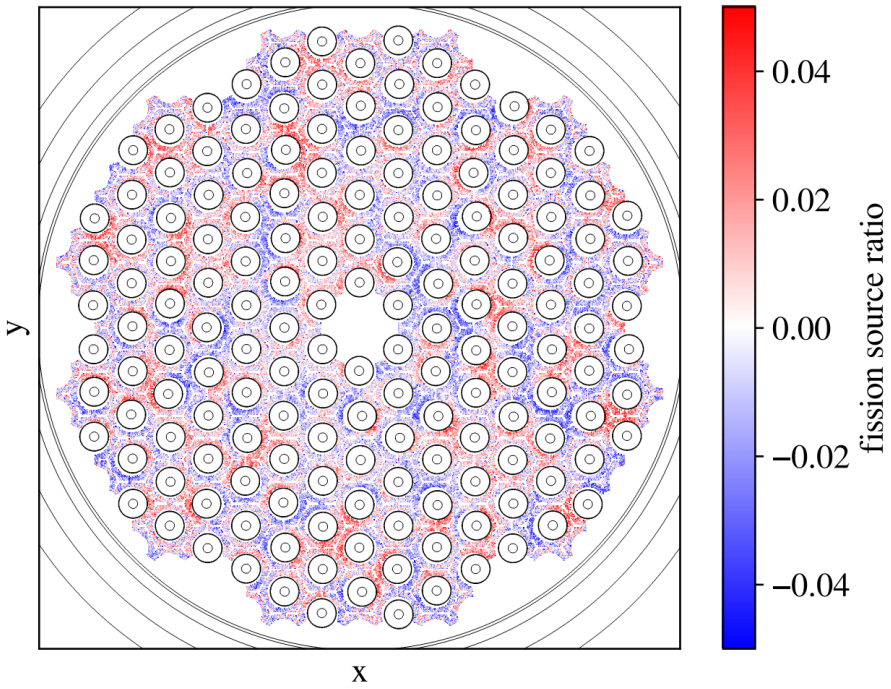

Figure 5. Relative difference in the fission source distribution between the nominal case and random moderator rod placement realization number 5. Red indicates that the random moderator rod fission source is higher than nominal, and blue indicates that the random moderator rod fission source is lower than nominal.

3.2. Thermomechanical Simulations Results

Contact along one fuel element tip and a corresponding larger gap along the opposite fuel element tip causes variation in the fuel-to-coolant heat transfer coefficients on those surfaces. Contact between fuel element tips has an insulating effect and lowers the heat transfer coefficient; conversely, a larger gap along the opposite fuel element tip yields a higher heat transfer coefficient than the as-designed gap. The effect on fuel element stress for these conditions is analyzed using a Bison fuel element model. The focus of this portion of the work is related to the overall fuel element and not the fuel performance of the individual TRISO particles in the compact. One identified accident scenario for a TCR nuclear demonstration included the failure of a fuel element resulting in a coolant channel blockage [8], so the focus of this work was on the overall fuel compact rather than the TRISO particles.

The heat transfer coefficients assumed for this work are provide in Figure 6. The heat transfer coefficient on the right side of Figure 6 (red surface) was set to zero to simulate contact with another fuel element, whereas the HTC on the left surface (orange surface) was set to 1.2× the nominal value. Figure 6 shows the coolant surfaces on the fuel element. The heat transfer coefficients were set to 1,382 W/m^2-K for the flat cog surfaces, 1,492 W/m^2-K for the outer curved surfaces, 1,540 W/m^2-K for the internal wishbone channels, and 1,445 W/m^2-K for the cylindrical moderator channel. The coolant temperatures were set to 804 K, 698 K, 702 K, and 696 K for the flat cog, outer curved surfaces, internal wishbone channels, and moderator channels, respectively. The heat transfer coefficients and the boundary temperatures are taken from the TCR preliminary design studies [2].

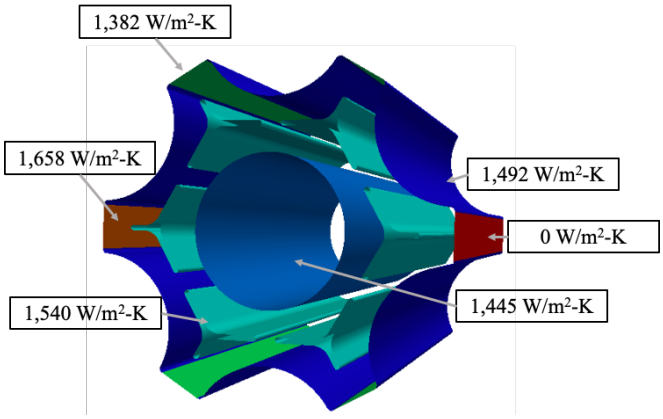

Figure 6. Representation of the coolant surfaces on the fuel element. The red surface on the right has a zero HTC, and the orange surface on the left has an HTC that is 1.2× that of the as-designed HTC, while the flat surfaces with as-designed HTC are shown as green.

The fuel elements were assumed to be constrained in such a way as to prevent displacements on the order of tens of μm using penalty Dirichlet boundary conditions which act like springs and sufficiently constrain the fuel element without inducing notable stress artifacts. No additional mechanical boundary conditions were added (i.e., friction or pressure from the neighboring contacting element was not modeled). The power was generated using true kernel locations determined from x-ray computed tomography postprocessing [5, 9], and the total power generated in the element was assumed to be 12 kW, corresponding to the average TCR fuel element. The resulting stress and temperature profiles are shown in the **Error! Reference source not found.** and **Error! Reference source not found.**. The lobe with a zero HTC is on the right, and the lobe with a 1.2× HTC is on the left. The temperature is about 40 K higher on the lobe with zero HTC. The stresses are also several megapascals higher than the other side with a 1.2× HTC.

The resulting temperature and stress profiles are shown in Figures 7 and 8. The lobe with a zero HTC is on the right, and the lobe with a 1.2× HTC is on the left. The temperature is ~40 K higher on the lobe with zero HTC, and the stresses are several megapascals higher than the side with a 1.2× HTC. However, the stresses on the lobe with a zero HTC remain less than those generated at the top and bottom ends of the fuel element. The stresses at the ends of the fuel element are caused by the lack of heat generation at the bottom and top surfaces of the element, which is caused by the solid SiC bottom surface of the fuel element and top overfill of SiC when filling the element. The lack of heat generation coupled with the coolant continuing to remove heat generate the larger stress at the element bottom and top surfaces.

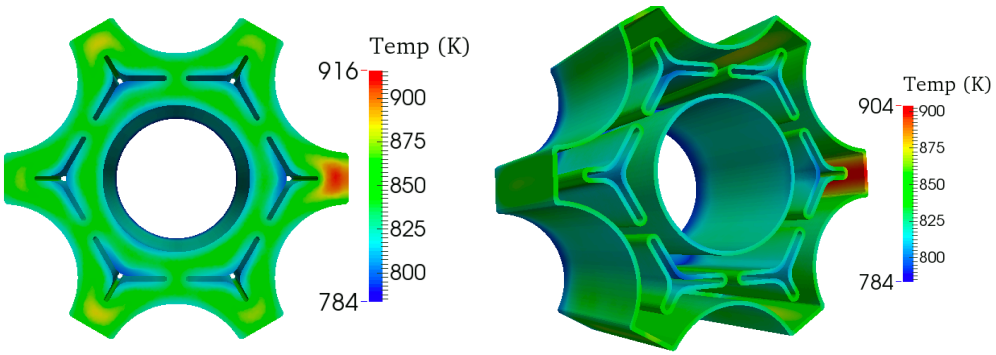

Figure 7. Temperature profile through the midsection of the fuel element (left) and surface temperature profile in the solid SiC fuel element shell (right).

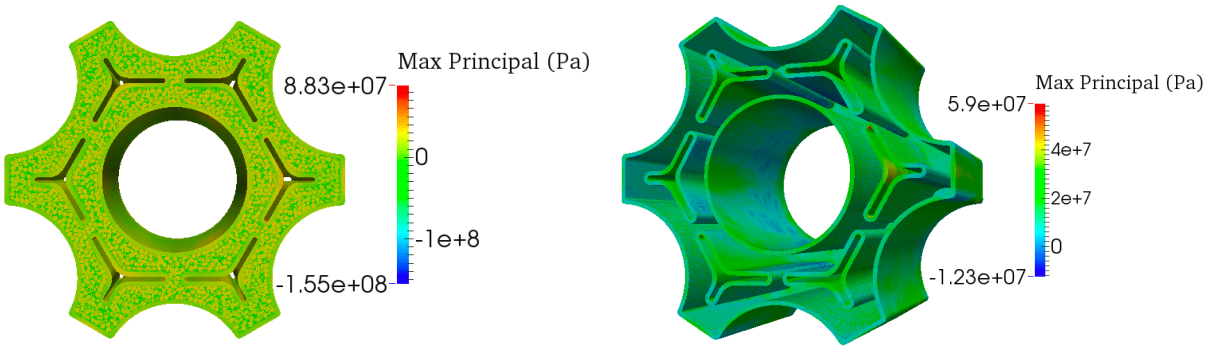

Figure 8. Stress profile through the midsection of the fuel element (left) and stress profile in the solid SiC fuel element shell (right).

The stress increase in the lobe with zero HTC is relatively small primarily because the lobe can expand without a large degree of constraint. The adjacent outer curved surfaces are colder and do not attempt to expand as much as the main portion of the lobe. However, the flat surface of the lobe is nearly as hot as the main portion of the lobe, and thus the expansion can occur without producing large stresses.

4. CONCLUSIONS

Under the TCR program in FY21, a full-core mock-up of the TCR preliminary design was completed and used to ascertain differences between the as-designed system and the actual printed and traditionally manufactured components in a full-core setting. Two selected deviations from the as-designed TCR core were selected for additional analysis and included variation in the moderator rod position and contact between fuel elements. Using a new layered geometry modeling capability in Shift, random rod placement was analyzed for neutronic impact. No significant effect on k_{eff} was found for the random movement of moderator rods; however, fission source—and, therefore, power—variation of up to +/-5% was observed. Bison was used to analyze the change in boundary conditions expected for fuel element contact, which resulted in insulating one fuel element tip while increasing the HTC in the opposite fuel element tip. Fuel element temperature and stress both increase in the fuel element tip that experiences contact. However, the temperature increase was well within the fuel failure limits, and the stress was lower than is experienced in the top and bottom of the fuel element under the as-designed conditions (i.e., consistent HTCs on all fuel element tips). These results indicate that the variations in the as-built nuclear core would not pose a significant risk to the safety of such a system. These results also suggest that further variability in the spacing of elements induced by irradiation over a longer operation would not significantly increase uncertainty in the core criticality or the fuel element failure probabilities.

ACKNOWLEDGMENTS

This work was funded under the US Department of Energy, Office of Nuclear Energy Transformational Challenge Reactor program, which has now transitioned into the Advanced Materials and Manufacturing Technologies Program.

REFERENCES

1. B. J. ADE et al., "Candidate Core Designs for the Transformational Challenge Reactor," *Journal of Nuclear Engineering*, **2** (1) (2021).
2. B. J. ADE et al., "Transformational Challenge Reactor Design Characteristics," *Proc. PHYSOR 2022 – Making Virtual a Reality*, Pittsburgh, PA, (2022).

3. K. A. TERRANI et al., "Architecture and properties of TCR fuel form," *Journal of Nuclear Materials*, 152781 (2021). http://www.sciencedirect.com/science/article/pii/S0022311521000040.
4. E. BIONDO et al., "Layered CAD/CSG Geometry for Neutronics Modeling of Advanced Reactors," *Proc. PHYSOR 2022 - Making Virtual a Reality*, Pittsburgh, PA, (2022).
5. B. ADE et al., "Particle Packing Characteristics in Dense TRISO/SiC Fuel Elements and the Impact of Neutronics and Thermomechanics," *Proc. Trans. Am. Nucl. Soc.* (2020).
6. "BISON: A Finite Element-Based Nuclear Fuel Performance Code," https://bison.inl.gov/SitePages/Home.aspx (accessed June 27, 2020).
7. D. SCHAPPEL et al., "Modeling Interface Debonding in Coated Fuel Particles with BISON," *Nuclear Science and Engineering*, 1-9 (2021). https://doi.org/10.1080/00295639.2021.1955590.
8. A. WYSOCKI et al., "Transformational Challenge Reactor Accident Analysis," Oak Ridge National Lab.(ORNL), Oak Ridge, TN (United States) (2020).
9. G. W. HELMREICH et al., "New method for analysis of X-ray computed tomography scans of TRISO fuel forms," *Nuclear Engineering and Design*, **357**, 110418 (2020). https://www.sciencedirect.com/science/article/pii/S0029549319304492.